Institute of
Space Sciences

EXCELENCIA
MARÍA
DE MAEZTU

ICREA

Radio pulsations from LS I 61 303

Diego F. Torres

Gamma-ray binaries hinted since the 1970's, studied since COS-B

Institute of Space Sciences

EXCELENCIA MARÍA DE MAEZTU

LS 5039

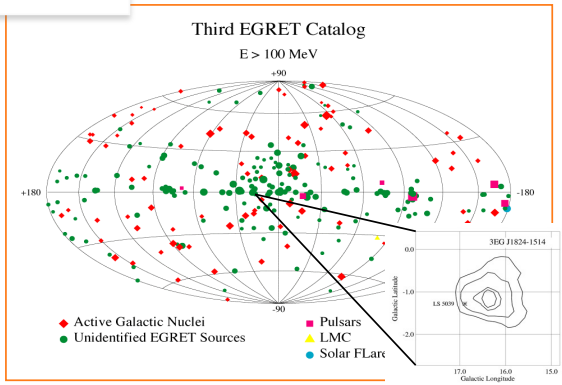

Paredes et al. 2000

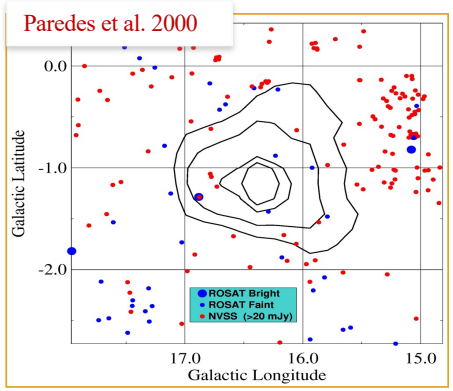

Paredes et al. 2000

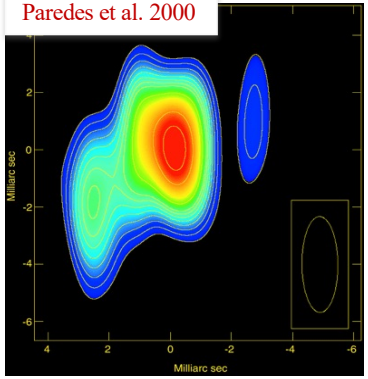

30/9/76 Hermsen

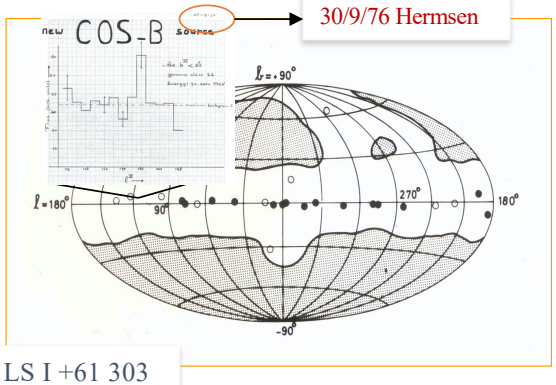

LS I +61 303

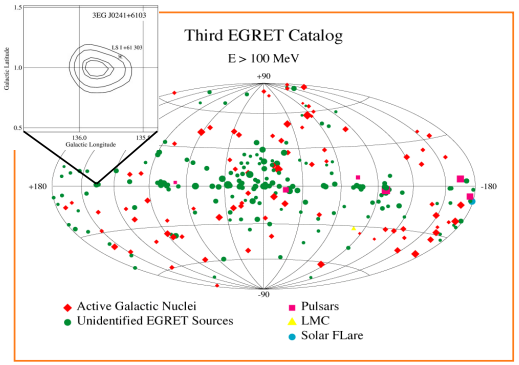

But none confirmed (orbital period) before Fermi.

No confirmed variability (orbital) // Bad positioning // many candidates in the field led these sources to remain unidentified.

A class defined by phenomenology, not nature

Institute of Space Sciences

EXCELENCIA MARÍA DE MAEZTU

Example: orbital variability of LS I 61 303 in TeV

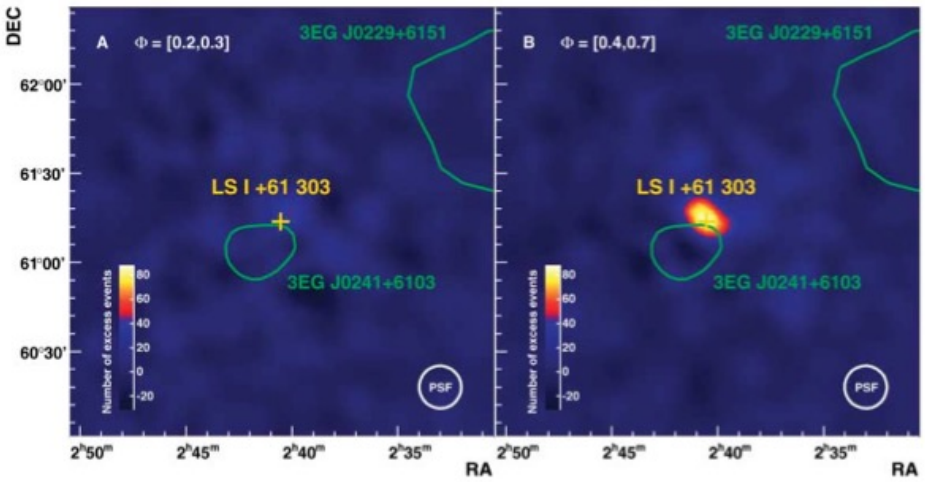

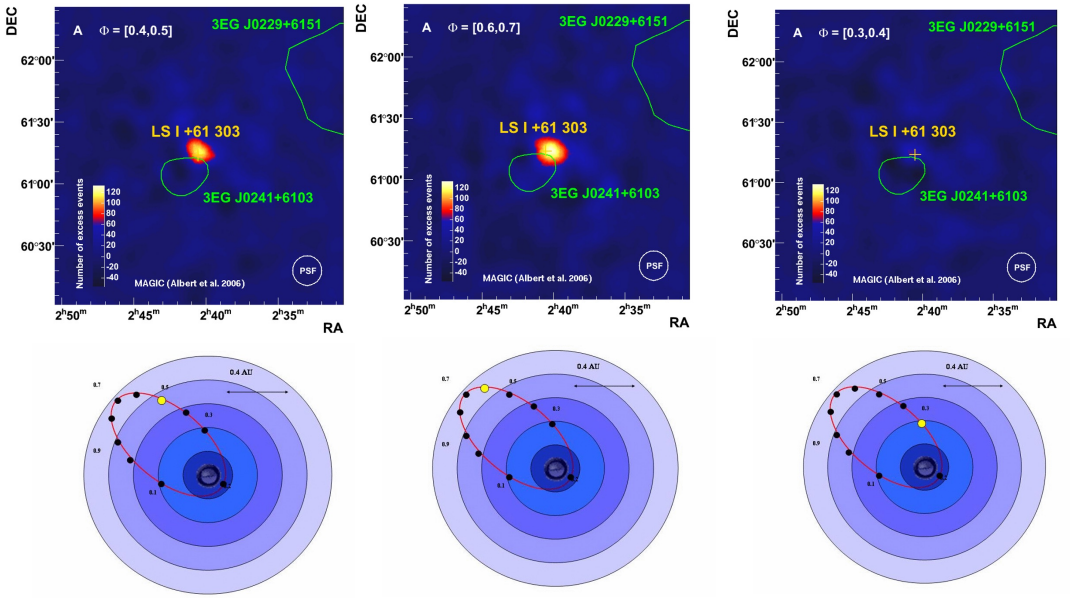

Extract from the initial 6 observations of the source

A class defined by phenomenology, not nature

-Not a very clear definition of the concept behind the name during a long time

2 main features:

-**gamma-ray emission above 10 MeV 'dominates'** the SED output

-Present **orbital variability across all frequencies**

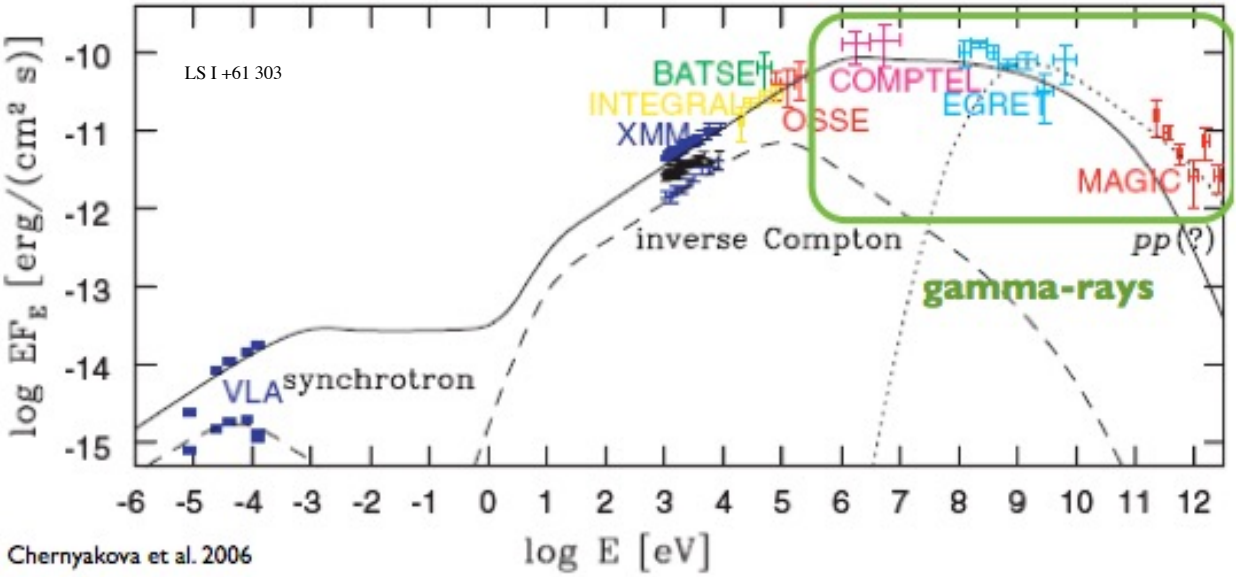

See e.g., Chernyakova et al. 2006, Dubus 2006

Variability shown with 4+ years of RXTE data

Institute of Space Sciences

EXCELENCIA MARÍA DE MAEZTU

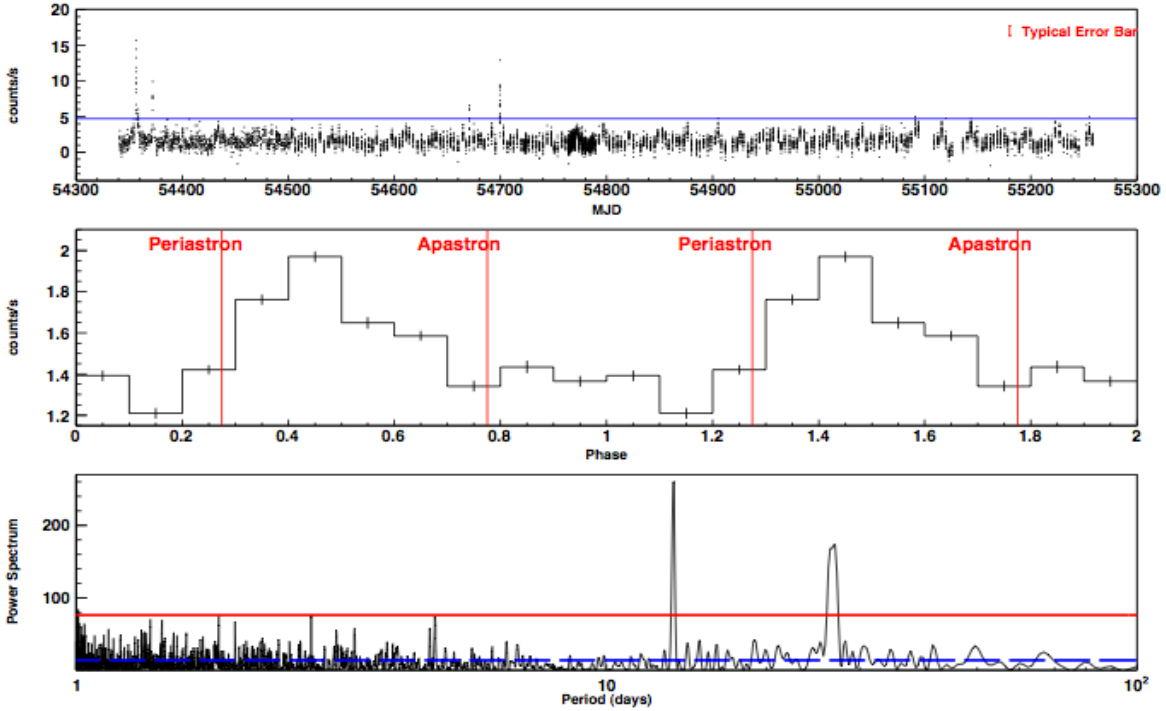

Fig. 1.— Top: Binned 3–30 keV lightcurve, with 64-second resolution, of the RXTE-PCA data of LS I +61° 303 from 2007 September to 2010 March. The horizontal line represents the upper flux cut considered in our analysis. Middle: Folded lightcurve with orbital ephemeris of LS I +61° 303 using the complete RXTE/PCA dataset. Bottom: Power spectrum of the whole RXTE-PCA data. The white noise (dashed line) and the red noise (solid line) at the 99% confidence level are plotted in the power spectrum.

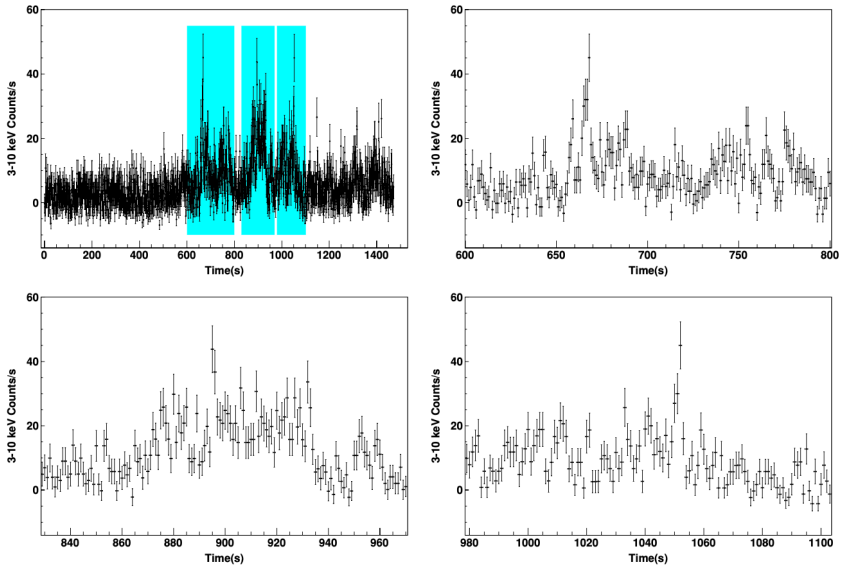

Inner structure of one of the flares, binned in timescales of 1 s to show internal structure. The three panels show the zoomed view of the colored part.

DFT et al. ApJ Letters 2010; Li, DFT, et al. ApJ (2011)

Variability shown with 4+ years of RXTE data

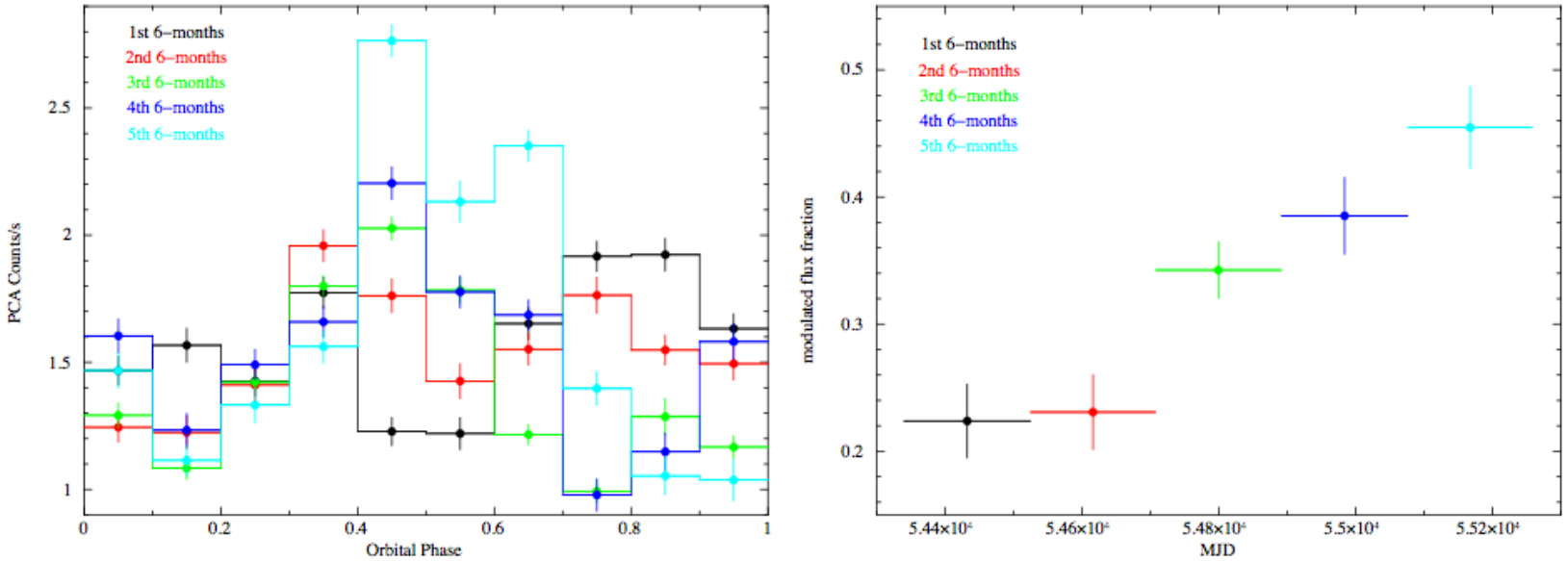

Note

1. that the lightcurves do not peak in the same place
2. that the average value increases, but slightly
3. that at fixed phase, there are significant flux variations (>7σ)

Discovering superorbital periodicity in X-rays

Institute of Space Sciences

EXCELENCIA MARÍA DE MAEZTU

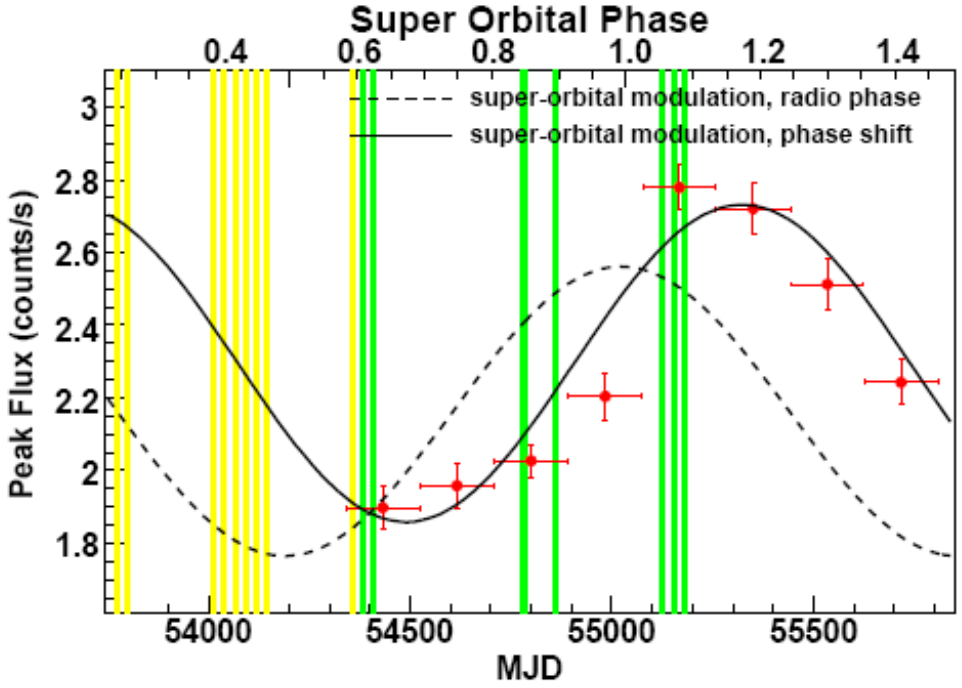

Dotted line: behavior in radio

Solid curve: sinusoidal fit to X-ray data (red) obtained with a fixed period to 1667 days

Green (yellow) boxes: TeV emission in low (high) state

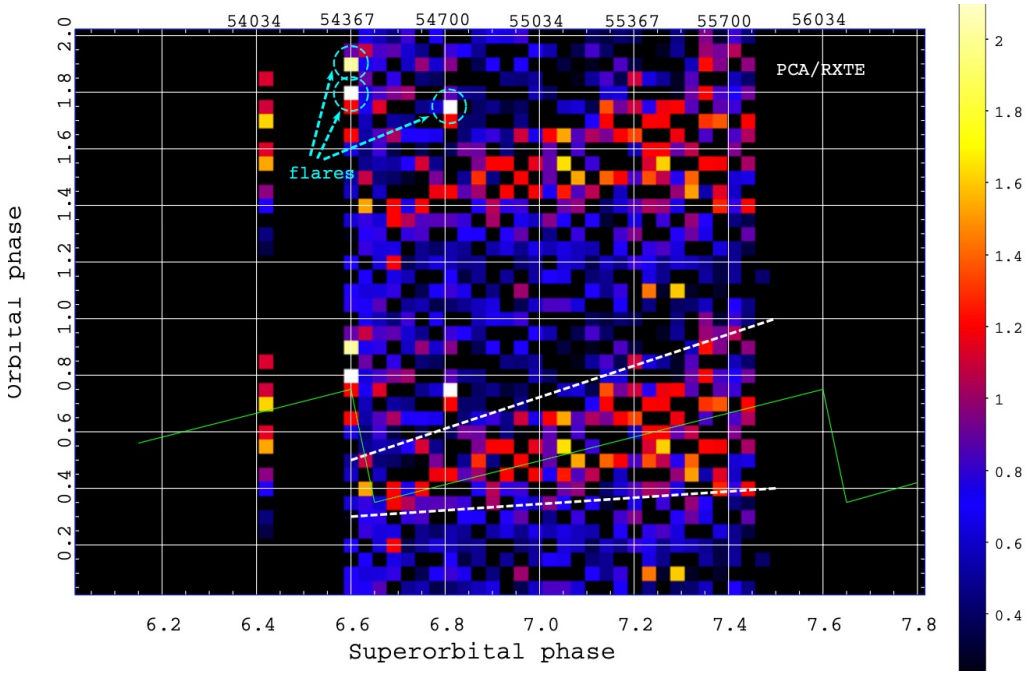

3–20 keV flux from LSI +61 303 as a function of the orbital vs. superorbital phase. The color scale is expressed in mCrab units.

Left: Li, DFT et al. 2012; Right: Chernyakova et al. 2012 (ApJ Letters, back to back articles)

... and superorbital periodicity in hard X-rays

Institute of Space Sciences

EXCELENCIA MARÍA DE MAEZTU

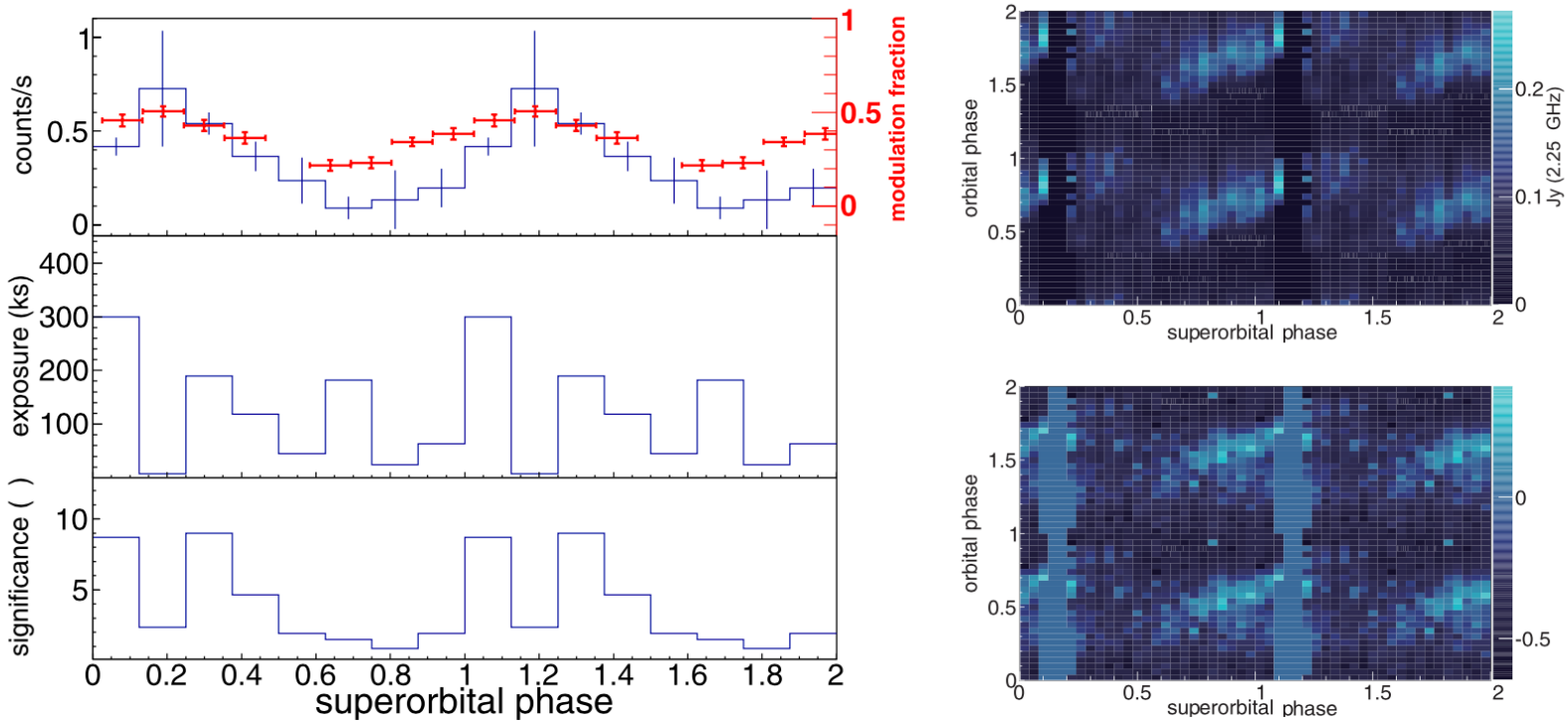

Figure 3. Left: superorbital light curve of LS I +61°303 in 18–60 keV, as observed by *INTEGRAL*. The red points show the modulated fraction in the 3–30 keV band from Li et al. (2012). Middle and bottom: exposure and significance for the corresponding superorbital phase, respectively. Right: radio flux intensity at 2.25 GHz (top) and spectral index (bottom) as a function of the orbital and superorbital phases.

The first Fermi detection of orbital periodicity

- LS I +61 303 location error radius of 1.8'
- consistent with the known position of the optical counterpart
- Flux variability is also clearly evident

variability

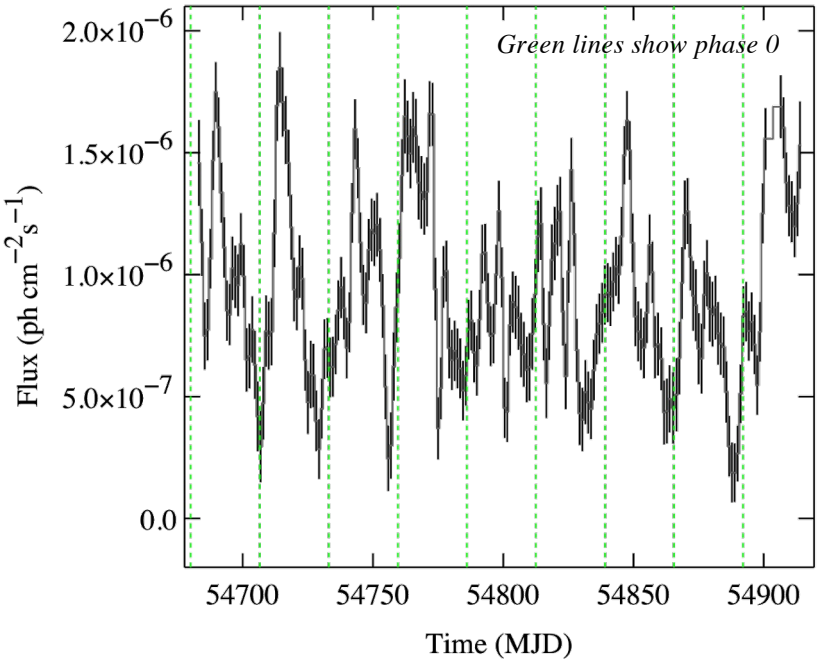

position

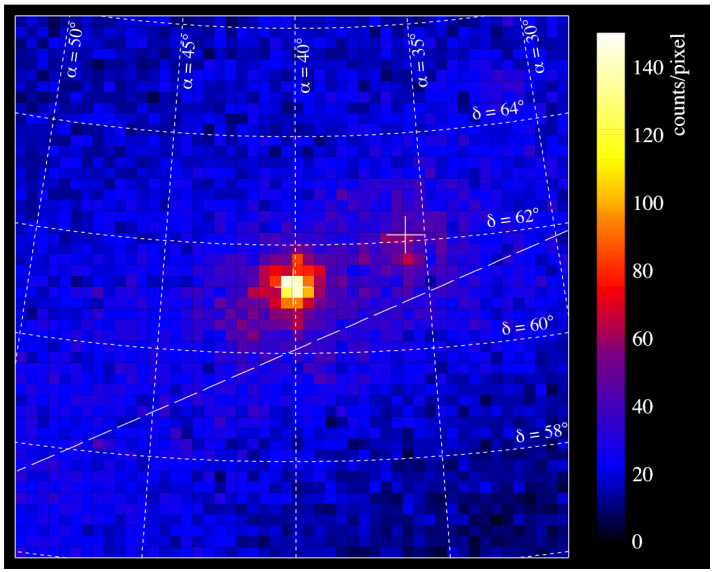

GeV long-term evolution: super-orbit

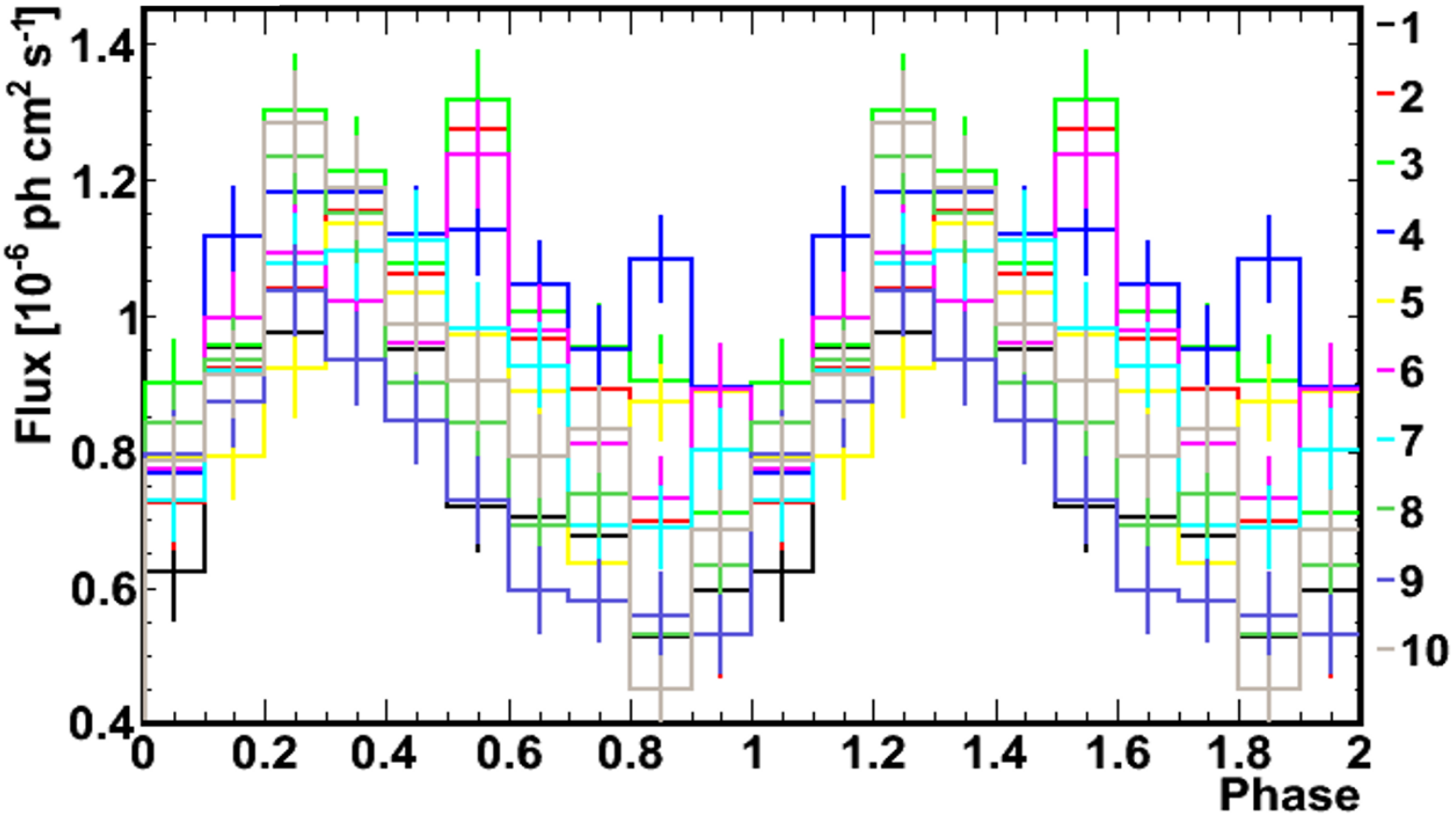

Ackermann et al. 2013, ApJ Letters (DFT corresponding author)

Separated in equal orbital phases, pattern seen

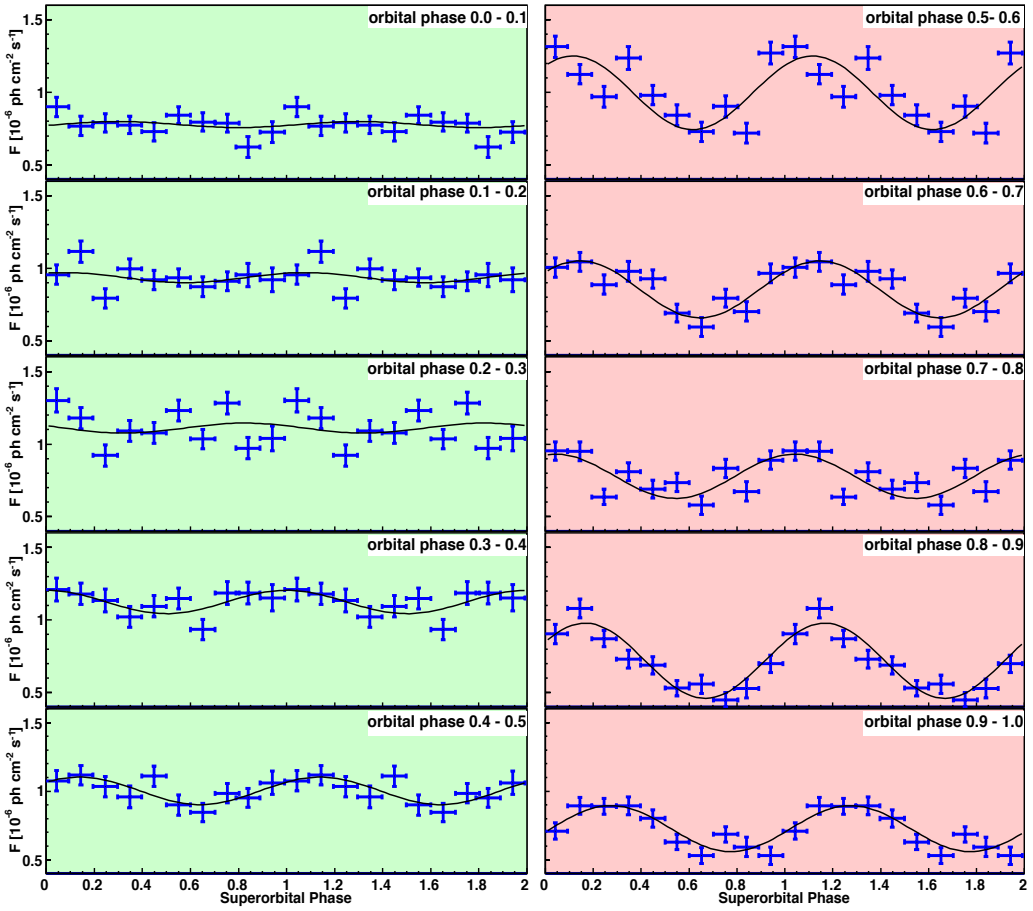

Each panel shows the GeV flux at a fixed orbital position (see labels), along a period of 4.5 years

The background represent the region of **periastron** and **apastron**, respectively

Black line: Sinusoidal fit with fixed superorbital period

Short magnetar flares

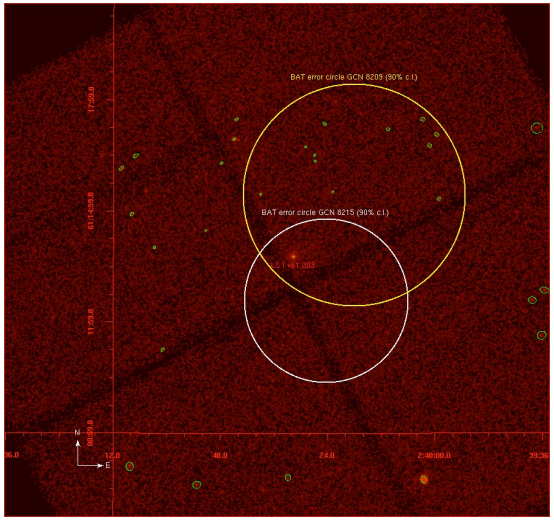

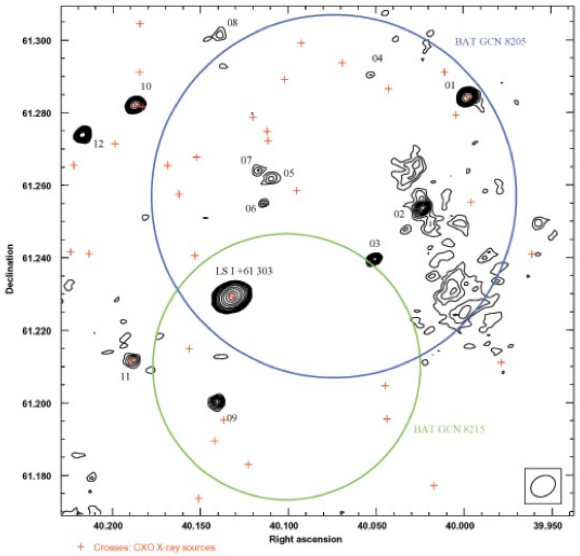

• On 2008 September 10th, Swift-BAT triggered on a short SGR-like burst from the direction of LS I +61 303.
• Swift-XRT did not detect the burst because started observing 921s after the BAT trigger.
• The burst location, lightcurve, duration, fluence, and spectra were fully consistent with a magnetar flare

• Archival analysis of Chandra ACIS-I observation showed many faint sources in the field of view, some with VLA detections (16 compact radio sources within a 10 arcmin field of view with a peak flux density above four times the rms noise).

•Magnetars are not usually associated with compact radio sources.
•Thus, any X-ray source without a radio counterpart within the field of view could in principle be the origin of the burst.

Initial claims at: GCN 8209, 8211, 8215; ATELs 1715,1731, 1740

Short magnetar flares

Institute of Space Sciences

EXCELENCIA MARÍA DE MAEZTU

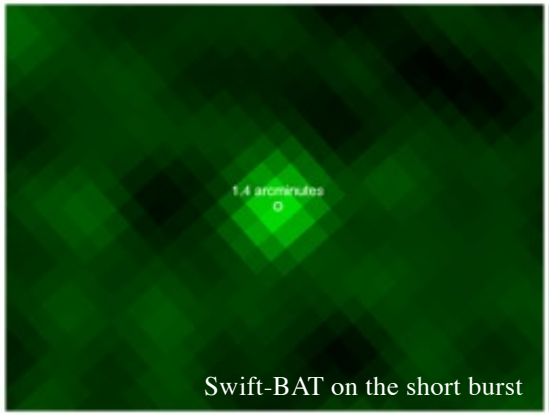

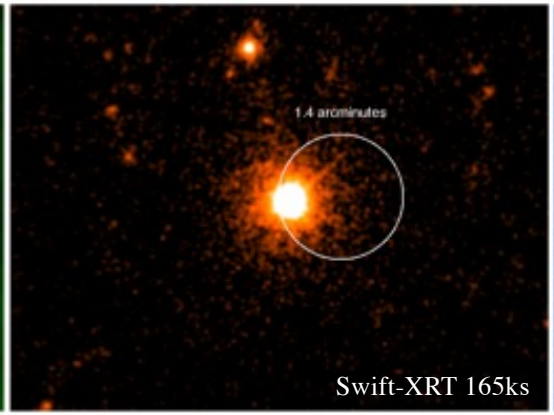

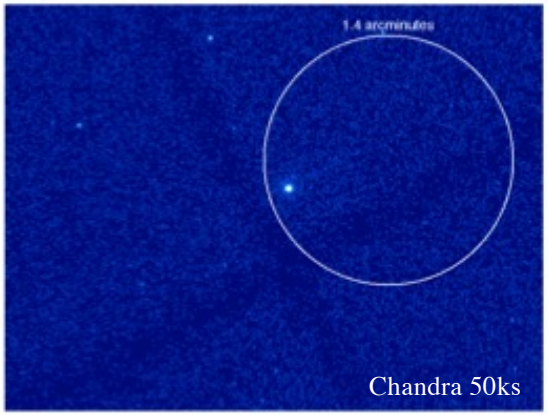

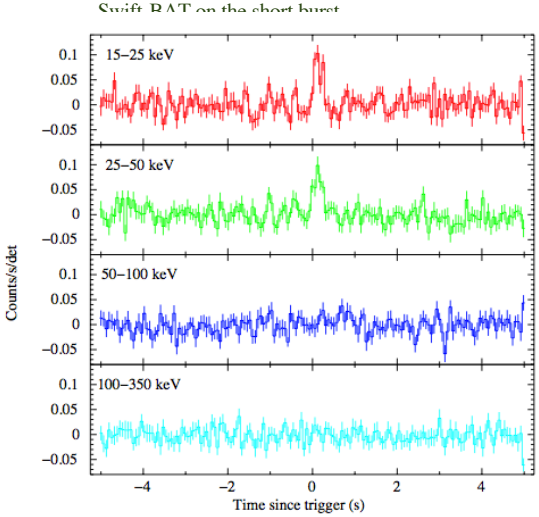

	PL	BB	Brems
Γ	2.0 ± 0.3	–	–
kT (keV)	–	$7.5^{+0.9}_{-0.8}$	43^{+32}_{-14}
R (Km)	–	$0.27^{+0.07}_{-0.05}$	–
Flux	5 ± 2	4.5 ± 0.7	4.5 ± 0.9
Fluence	1.4 ± 0.6	1.4 ± 0.2	1.4 ± 0.3
χ^2/dof	1.29/14	1.07/14	1.22/14

NOTE. — *Swift*–BAT spectroscopy in the 15–50 keV energy range. Errors are at a 1σ confidence level for a single parameter of interest. Fluxes and fluences are in the 15–50 keV energy range and in units of 10^{-8} erg cm^{-2} s^{-1} and 10^{-8}erg cm^{-2}, respectively. The blackbody radius is calculated at infinity and for a distance of 2 kpc (which is the distance to LS I +61°303; Frail & Hjellming (1991)).

Table 1
Bursts Observed by *Swift*-BAT from LS I +61°303

	Burst No. I[a]	Burst No. II[b]
Date	2008 Sep 10	2012 Feb 5
Position uncertainty	2′.1	3′
Angular separation	0′.60	1′.07
T_{100} (s)	0.31	0.044
Fluence (10^{-8} erg cm^{-2})	1.4 ± 0.6	0.58 ± 0.14
Γ	2.0 ± 0.3	3.9 ± 0.4
Luminosity (10^{37} erg s^{-1})	2.1	6.3

Notes. The positional uncertainty is given at a 90% confidence level, including also systematic uncertainties. The angular separation is calculated with respect to the position of the optical counterpart. The T_{100} duration and the fluences are estimated in the 15–50 keV band. Burst spectra were fitted by a power law with index Γ. The average luminosity is estimated by assuming a distance of 2 kpc (Frail & Hjellming 1991).

[a] Torres et al. (2012).

[b] From Burrows et al. (2012); see also http://gcn.gsfc.nasa.gov/notices_s/513505/BA/.

DFT, et al. 2012

Searching for pulsations in X-rays, UL only

LS I +61 303

95 ks Chandra observation near apastron

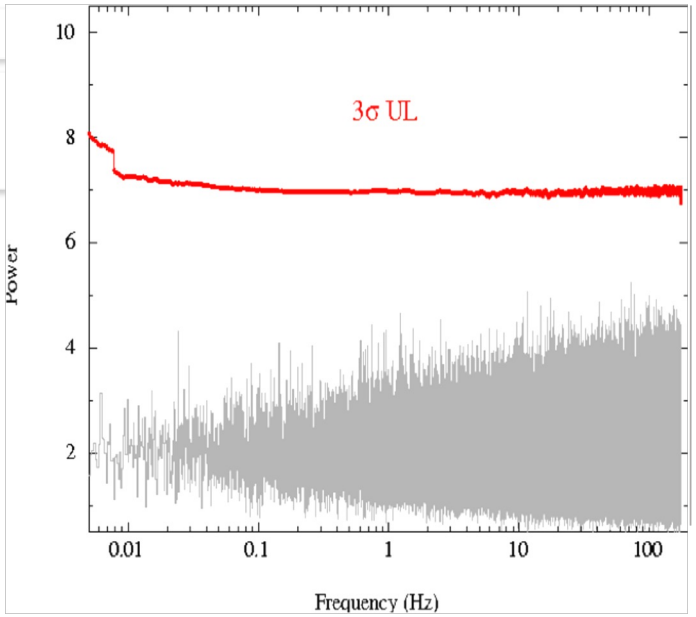

Pulsed fraction 3σ UL on the semi-amplitude of a sinusoidal signal

• Search for periods with frequencies 0.005 – 175 Hz (timing resolution of the CC-mode: 0.00285 s)

• Pulse fraction upper limits between 7 – 15 % for the whole energy range (larger in smaller energy bands); does not add much, several known pulsars have similar upper limits

Not in lack of reasons for the absence of pulses

Searches in the radio, X-ray, hard X-rays, and gamma-ray band were not successful in finding pulsations.

- **In radio,**

free-free absorption -which may have a complex temporal behavior according to binary conditions- can wash out the pulses, and/or the radio cone of emission may altogether point in a different direction from Earth.

- **In X-rays,**

a pulsed fraction upper limit of ~10% is normal, could well be larger than the actual pulsed fraction of the source as is the case for other pulsars. Only a few dozen pulsars out of the ~ 300 detected in gamma rays and the ~ 3000 in radio have non-thermal X-ray pulsations detected.

- **In gamma-rays,**

1) LS I +61 303 lies in a **complex region**, and not only the diffuse background, but the likely origin of at least part of the GeV emission beyond the magnetosphere of the putative pulsar may preclude detecting pulses.
2) the **uncertainty in the orbital parameters** reduces the sensitivity of blind searches across all frequencies when long integration times are needed

If no pulsations, nature is never certain

- Consider the accreting binary 4U 1700-37,
  - A very similar HMXB to LS 5039 (i.e., similar companion star and 4-days orbital period, but no TeV emission) located at ~ 1.5 kpc

- Left: XMM-Newton spectrum of 4U 1700-37 (first published by van der Meer et al. 2005).
- Right: how would these accretion lines look, assuming all are present, in the available data for LS 5039

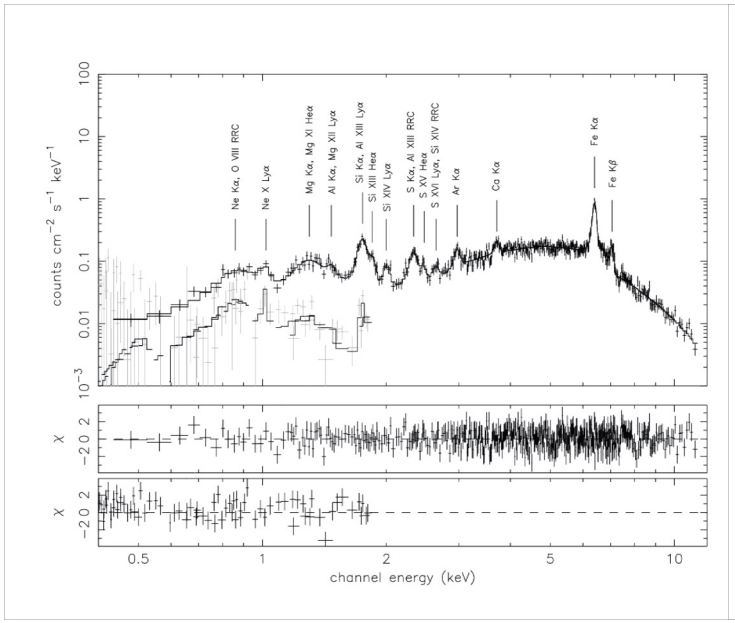

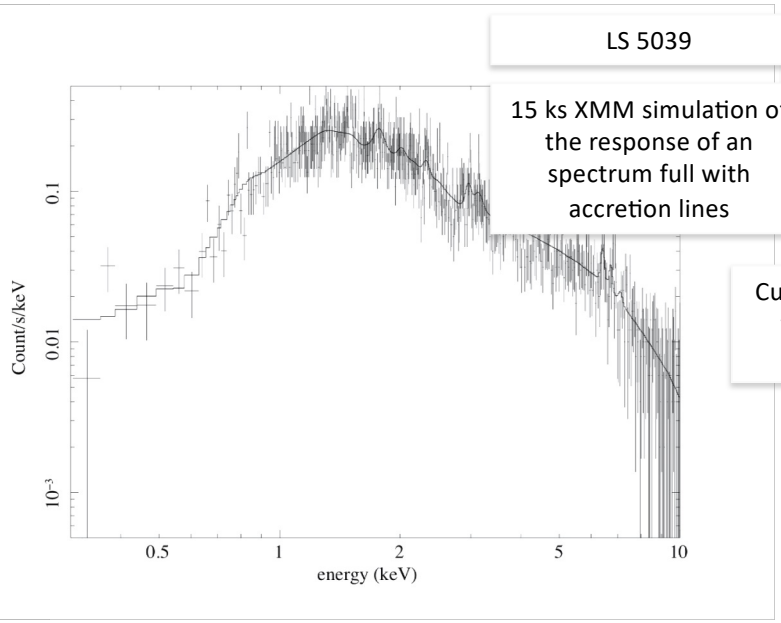

Rea, DFT et al. 2010, ApJ

Radio pulsations discovery

FAST: observing at larger radio sensitivty

- The best chance to detect pulsations from LS I +61 303 was to try observing at a large radio sensitivity in the orbital region where the free-free absorption effect due to the stellar wind (or disk) would naturally be the lowest (see e.g., Cañellas et al. 2012)

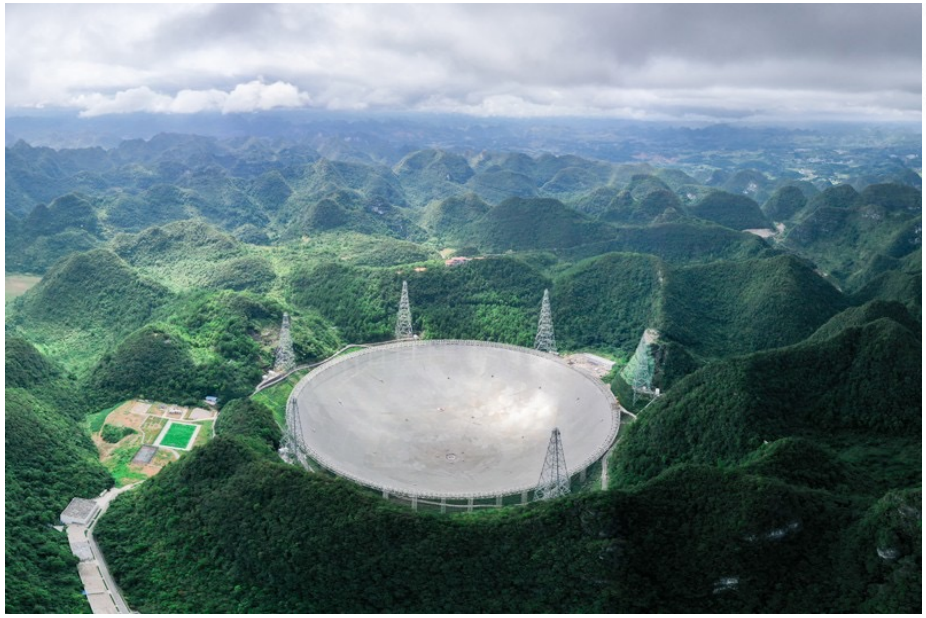

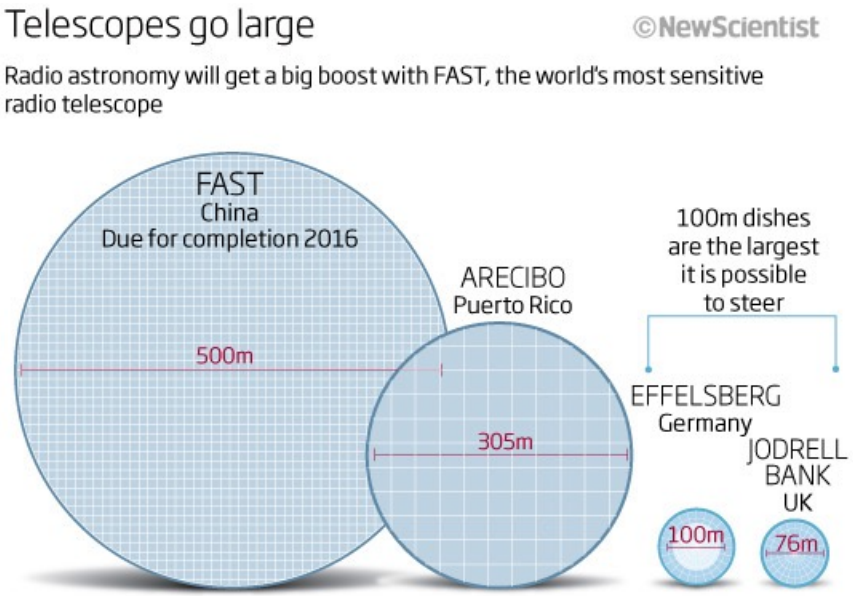

The advent of FAST

- FAST: 500 meters, single dish, ~10 better sensitivity than Arecibo.
- Constructed in 2016, operated since 2019.

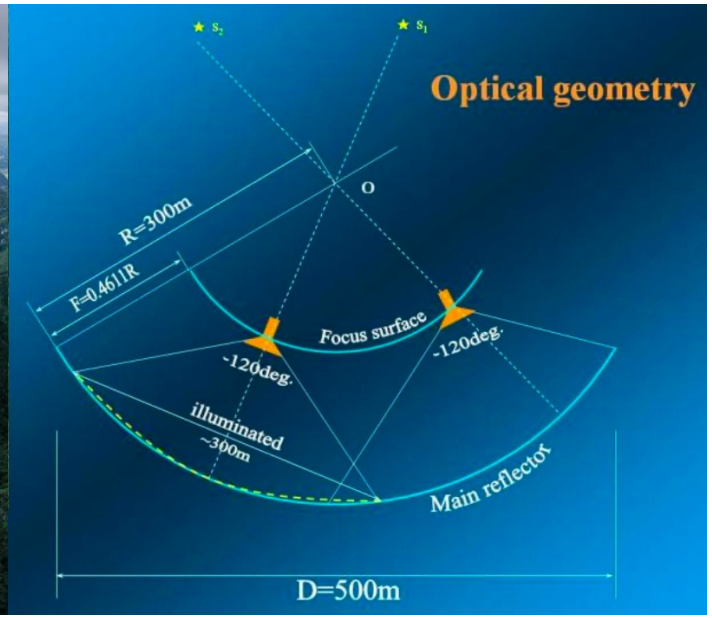

FAST chase of LS I + 61 303

- We tried observing LS I 61 303 since risk-shared time was available in FAST
- We finally obtained data in 2019-2020.
- At the time, there was no unusual behavior displayed in survey data, including Swift/BAT, MAXI, and *Fermi*-LAT. We also checked on other X-ray and gamma-ray data, but found no obvious signal at the period.

We had a total exposure time of ∼ 10.2 hours: one at the orbital phase of ∼ 0.07 and three around the orbital phase of ∼ 0.6. The zero of orbital phase of LS I +61 303 is defined at MJD_0 = 43, 366.275, and the orbital period is estimated as P = 26.4960 days, assuming the orbital phase of periastron is ϕperi = 0.2317 from Aragona et al. 2009.

	Mid of observation time	Orbital phase	Exposure Time/h	Sampling Time/μs	Pulse detected	$S_{mean}/S_{UL}/\mu$Jy
11-01-2019	58,788.7257	0.07	2.2	98.304	No	–/1.61
01-07-2020	58,855.5278	0.59	3.0	98.304	Yes	4.40/1.37
09-01-2020	59,093.8646	0.58	3.0	196.608	No	–/1.37
09-02-2020	59,094.8681	0.62	2.0	196.608	No	–/1.68

Radio pulsations recorded: P~0.27 s

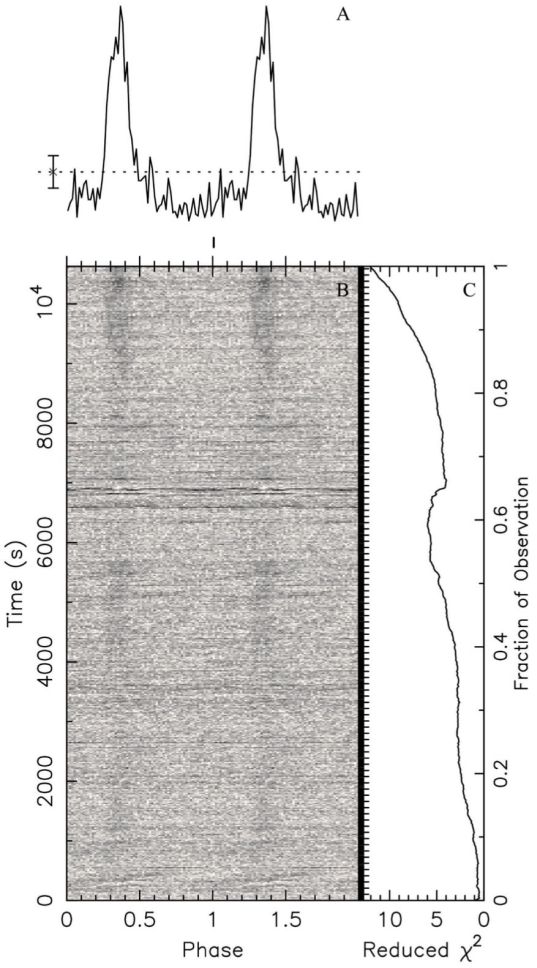

- **An unambiguous pulse signal (~22.4σ) with a single-peak profile emerges from the data taken on 2020 January 7th (MJD = 58,855.5278, 2020 January 7).**
- **The period, pulse width and DM of this pulsar are 269.15508(16) ms, 33.30 ± 0.96 ms, and 240.1 pc cm−3, respectively**
- The pulsations disappeared in the 3rd and 4th observations (one-day apart of each other), taken several months after the positive detection, at a similar orbital phase.
- A single pulse search was conducted for our observation, and more than 40 were detected in the second observation (where the radio pulsation is visible), but none were seen in the other three (see Methods).
- Given that our observations are short in comparison to the orbital period of the binary, and the pulsation appears to be non-steady in nature, the orbital imprint cannot be detected in our data.

Details of radio pulsations recorded

Institute of Space Sciences

EXCELENCIA MARÍA DE MAEZTU

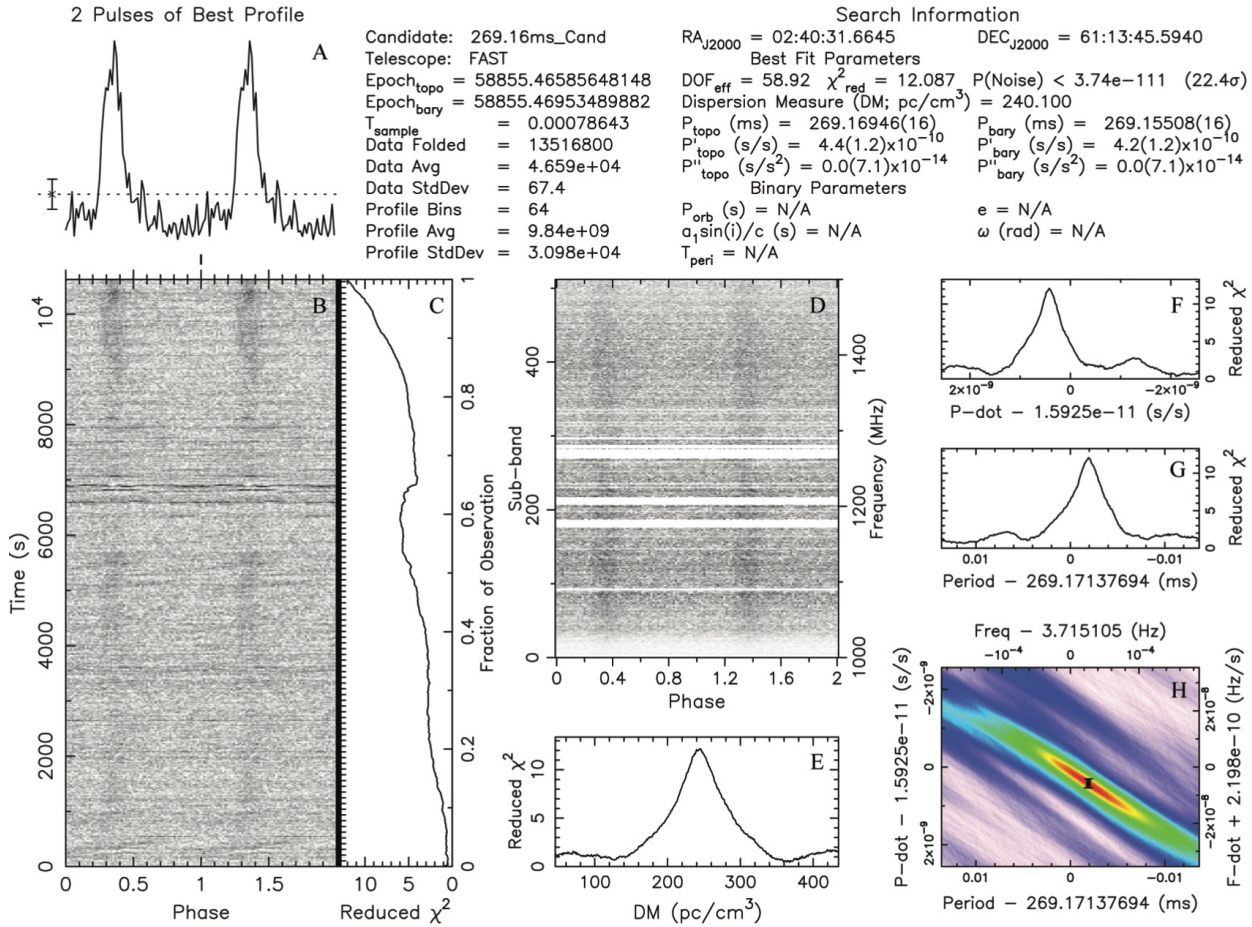

- Standard plot of the radio-pulsation search results with the routine prepfold in the PRESTO package.
- The validity of derived parameters can be found in the panels E-G
- The confidence contour of P and dotP is shown in H.
- The averaged pulse profile as a function of observing frequency is shown D. Pulse profile is shown in A.
- Pulse profiles are shown in the left-hand plots.

Many single pulses detected from LS I + 61 303

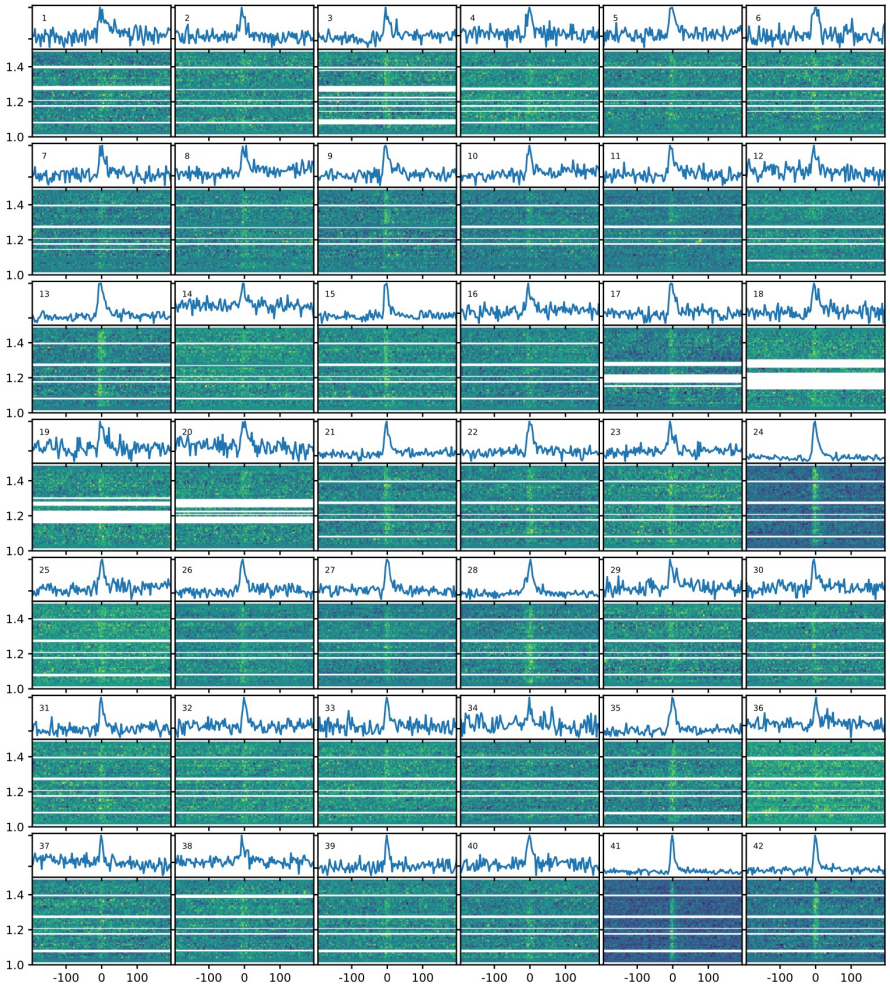

- **Single pulses detected in the *FAST* data for 2020 January 7.**

- The profile of the single pulse varies from each other, as is commonly found in other pulsars.

Single pulses detected all along the 2nd obs.

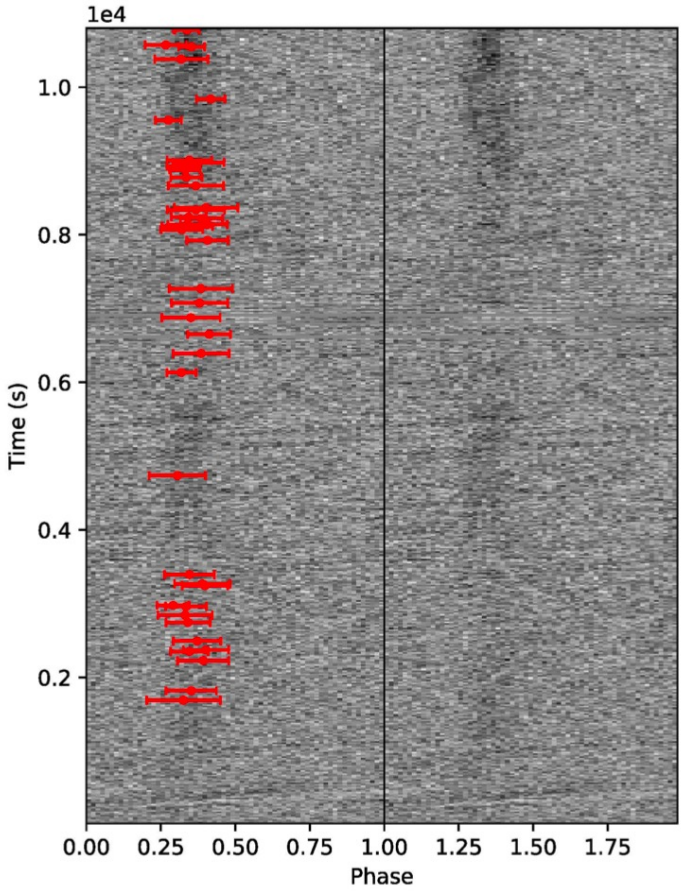

- The intensity versus the pulse phase and the observational time.
- The red bars mark the pulse phase and the occurrence time of the single pulses having a S/N ratio larger than 7. Many others seen.

Rapid changes of conditions

The fact that the pulsations are not present in three out of four observations (a couple of them very close to one another) reveals a rapid change of conditions either in the interstellar medium between us and the source, the neutron star environment, or the neutron star itself.

Scintillation

Nulling

Variable absorption

Rapid changes of conditions: scintillation

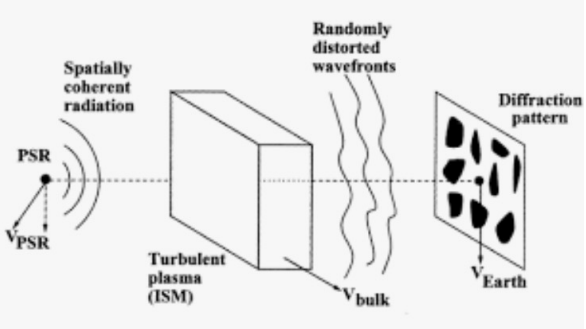

- Scintillation is unlikely:

$$\Delta t_d = 2.53 \times 10^4 (D\Delta\nu_d)^{1/2}/(\nu V_{\rm ISS})\ {\rm s},$$

- could explain changes in flux up to a few minutes, but not the several hours, in consecutive days, when pulsations are absent.

Diffractive scintillations occur over typical timescales of minutes to hours and radio bandwidths of kHz to hundreds of MHz, and they can cause more than order-of-magnitude flux-density fluctuations. **Refractive scintillations** tend to be less than a factor of ~2 in amplitude and occur on timescales of weeks.

Rapid changes of conditions: nulling?

More than 200 radio pulsars have been already seen to experience nulling (~8% of the sample).

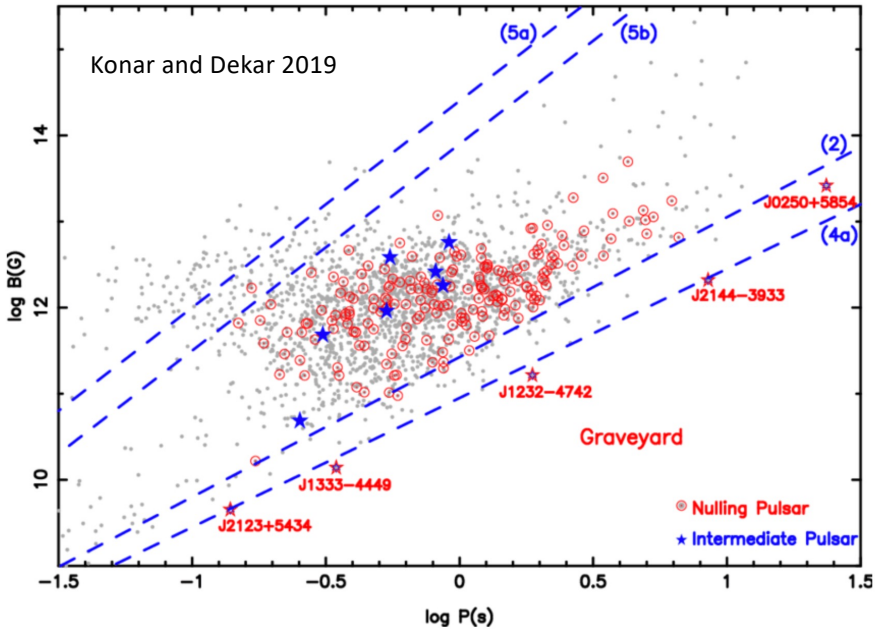

Observed radio pulsars and theoretical death-lines in the P s -B s plane. Top Panel: The death lines have been marked according to their numbering in the text. Bottom Panel: Nulling pulsars and intermediate pulsars have been highlighted with a small subset of death-lines. A number of pulsars have been specially identified (red open star) which appear to be functioning beyond the least stringent death line. The data for the known pulsars have been obtained from the ATNF pulsar cataloghttp://www.atnf.csiro.au/research/pulsar/psrcat/ (Manchester et al. 2005).

- The null fraction (the total fraction of pulses without detectable emission) and the null length (the duration of a nulling episode) exhibit a wide range of values
  - the null fraction goes from just a few % to over 90%,
  - the null length goes from a few single pulses to a complete disappearance of the emission for years at a time.
- Extreme intermittent pulsars exist where nulling can last from days to years, for example - J1933+2421 (Kramer et al. 2006a), J1832+0029 (Lorimer et al. 2012), J1910+0517 & J1929+1357 (Lyne et al. 2017).
- Also similar to RRATs, pulsars which sporadically emit single pulse outbursts instead of continuous pulse trains

Plot from Konar and Dekar 2019

Rapid changes of conditions: absorption?

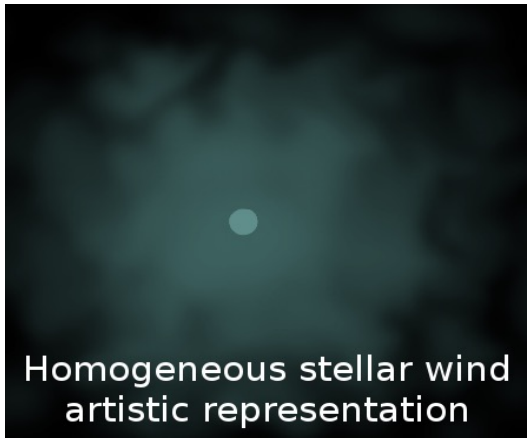

Homogeneous stellar wind artistic representation

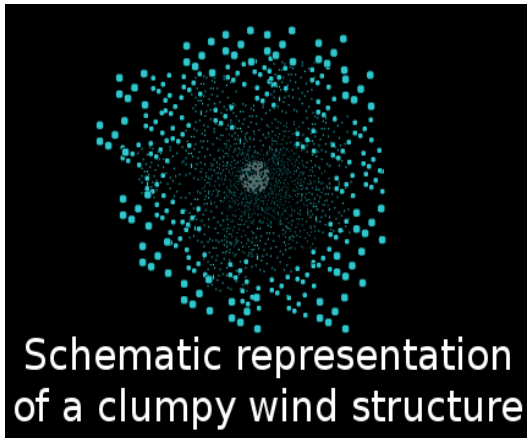

Schematic representation of a clumpy wind structure

- Changes in the wind properties can easily affect the pulsed signal. And as the Be stellar wind is likely to be clumpy, it would be impossible to predict the absorption level that any radio signal will be subject to in a local basis. Then, the transient behaviour could plausibly be interpreted as a result of the rapid change in the environmental conditions.
- Similar to the gamma-ray binary PSR B1259-63. Despite this system has a much larger orbit, radio flux variations at a time scale of minutes to hours were also reported, together with changes in the local properties of the Be star wind/disk encountered by the pulsar.
- It is reasonable to expect these same effects apply to LS I +61 303, enhanced due to the smaller spatial scale of the system.

Period consistent with young, energetic system

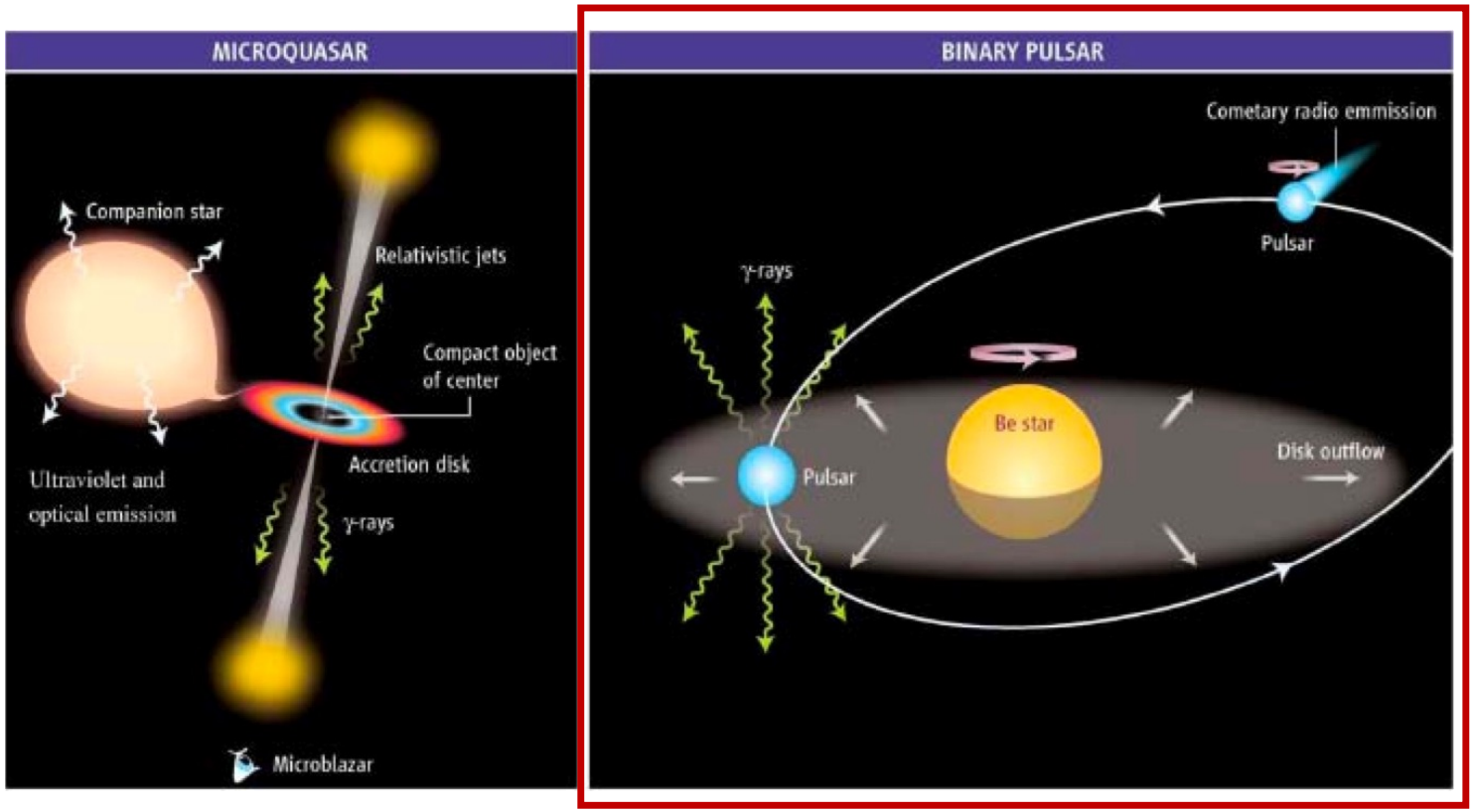

Plot from Mirabel 2006

In the right range for flip-flop

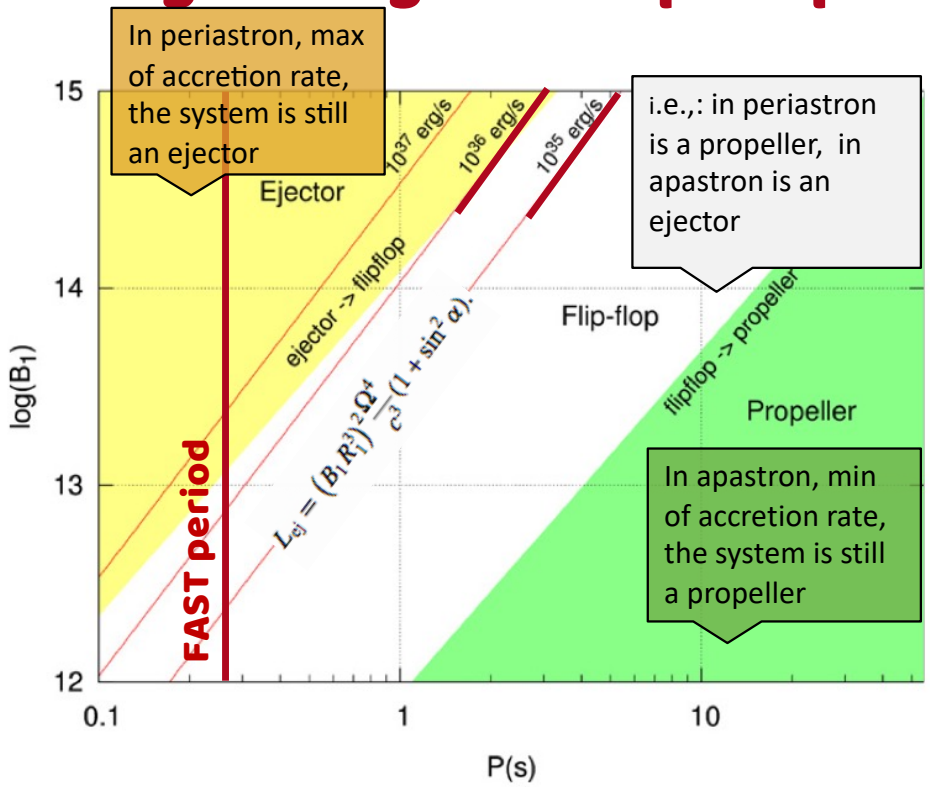

Figure 6. Ejector, *flip-flop*, and propeller states plotted in the NS magnetic field vs. spin period phase space, evaluated for a NS in LS I +61°303 and for the fiducial values adopted for the maximum and minimum mass capture rate ($\dot{m}^{\max} = 1, \dot{m}^{\min} = 1$). From top to bottom, the red solid lines mark the relation between the period and the magnetic field of the NS when the ejector luminosity is 10^{37}, 10^{36}, and 10^{35} erg s^{-1}, respectively, and the magnetic offset angle is $\alpha = 45°$.

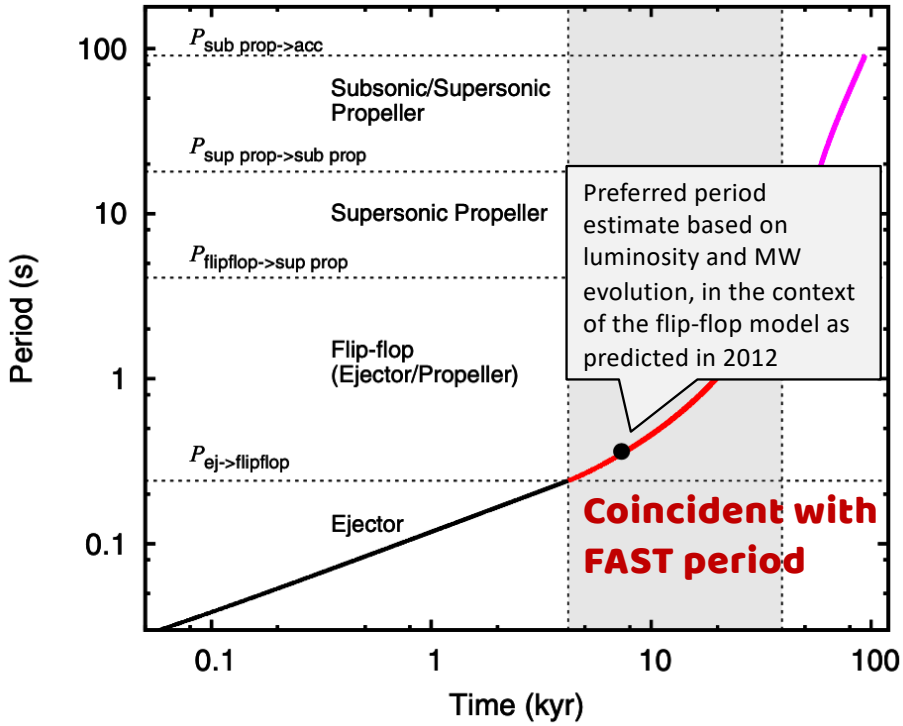

Figure 4. Evolution of the spin period of a NS in a system such as LS I +61°303, obtained considering the fiducial values of the system parameter (see Table 2). Dashed horizontal lines mark the transition among different states, while the gray shaded area marks the time interval during which the NS is expected to lie in the *flip-flop* state. The black filled circle marks the spin period at which the system emits an ejector luminosity of 5×10^{35} erg s^{-1}.

Plots from Papitto, Torres, Rea, ApJ 2012

Conclusions

Changing the mystery..

- LS I 61 303 is a pulsar-composed system with P=0.27 s.
- Actually, LS I 61 303 is the first system containing a pulsar behaving as a magnetar, probably one of the low-field magnetars class.
- The period found is consistent with the flip-flopping system: it is right at the spot that is better suited to qualitatively explain the MW behavior.
- The pulsar turns ON and OFF, and appears to be OFF a significant amount of time.
- Subsequent concurrent radio/X-ray observations are ongoing (NICER, FAST, et al.). Period redetected already, but again, not at all times.
- Aim is no longer to determine the nature of LS I 61 303 but to understand better the cause of the turning off of the pulsar, and characterize its behavior.

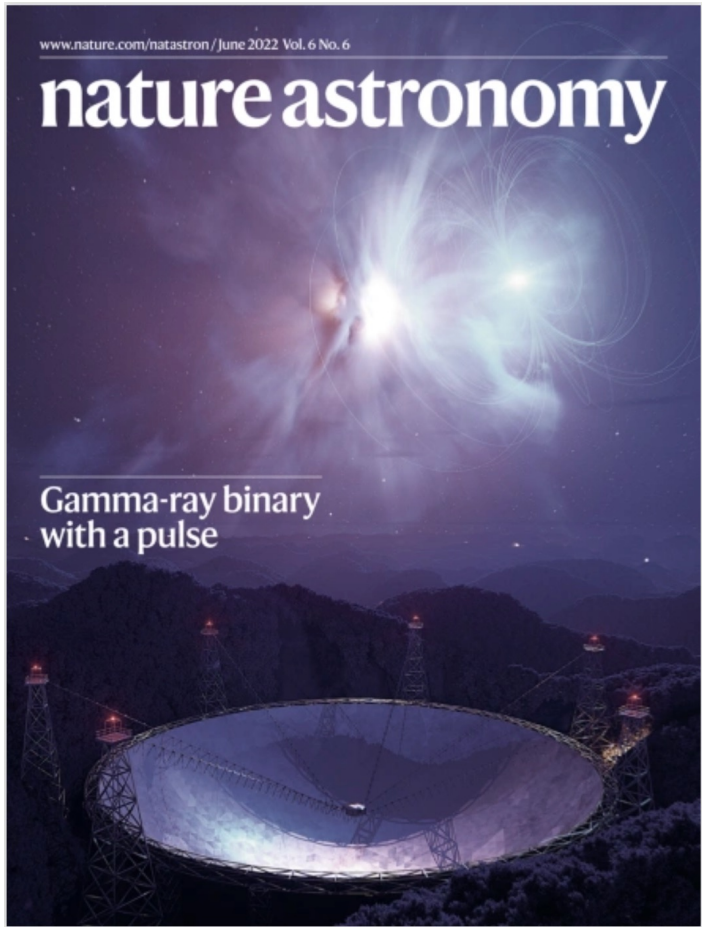

Thank you

https://sites.google.com/view/dft-research

@dft_research

GOBIERNO DE ESPAÑA
MINISTERIO DE CIENCIA E INNOVACIÓN

CSIC
Institute of Space Sciences

EXCELENCIA MARÍA DE MAEZTU

ICREA

Extra slides

https://sites.google.com/view/dft-research

@dft_research

GOBIERNO DE ESPAÑA
MINISTERIO DE CIENCIA E INNOVACIÓN
CSIC
Institute of Space Sciences
EXCELENCIA MARÍA DE MAEZTU
ICREA

FAST estimate of mean flux density

- An estimate of the mean flux density that each of our observations would have detected, S_{mean}, can be obtained as

$$S_{\rm mean} = \frac{\eta\beta T_{\rm sys}}{G\sqrt{N_{\rm p}\Delta\nu T_{\rm int}}}\sqrt{\frac{W}{P-W}}$$

where η is the SNR threshold, β is the sampling efficiency, T_{sys} is the system temperature, T_{int} is the integration time, and G represents for antenna gain.

- For *FAST*, β=1, T_{sys}=24 K, G=16 K Jy^{-1}., the bandwidth is 300 MHz –after masking to remove RFI-, Np = 2 is the number of polarizations, P is the period of pulsar, and W is the width of pulse profile. The value of W/P =0.1 is adopted for LS I 61 303.

PRESTO analysis

1. We masked and zapped the radio-frequency interference (RFI) using the routine rfifind;

2. After RFI excision, the data were de-dispered with the trial DMs between 0 and 500 pc cm−3 by using the routine prepsubband;

3. For the resulting de-dispered time series, we carried out a blind Fourier-domain acceleration periodicity search with the routine realfft and accelsearch, yielding the periodic candidates.

4. The periodic candidates were further sifted with the routine ACCEL sift.py.

5. The data were corrected to Solar System Barycentre and were automatically folded over all derived periodic candidates and possible period-derivatives using the routine prepfold.

FAST chase of LS I + 61 303

Pulse No.24 and Pulse No.41 show an exponential-like scattering tail. For these two bursts, we used a Gaussian convolved with a one-sided exponential function to fit them,

$$f(t,\tau) = \frac{S}{2\tau}\exp\left(\frac{\sigma^2}{2\tau^2}\right)\exp\left(-\frac{t-\mu}{\tau}\right) \times \left\{1+\mathrm{erf}\left[\frac{t-(\mu+\sigma^2/\tau)}{\sigma\sqrt{2}}\right]\right\}$$

S is the flux density of the Gaussian, μ is its center, and σ is its standard deviation. τ is a time constant of the one-sided exponential function. We split the data into 8 evenly spaced sub-bands across the 500 MHz raw bandwidth, then clip the channels RFI.

For each sub-band with SNR ≥ 7, we integrated the pulse intensities over time and fit the intensity profile with the equation above along the frequency axis in order to get the scattering time scale (σ_{chn}) and the standard deviation (τ_{chn}) of each sub-band. At each frequency channel, the scattering time scale is

$$\tau_{\mathrm{chn}}(\nu) = \tau_{\mathrm{chn}}\left(\frac{\nu}{\nu_{\mathrm{ref}}}\right)^{\alpha}$$

where ν_{ref} is the reference frequency and is set to 1 GHz, α is the frequency scaling index

Detail on pulse #24

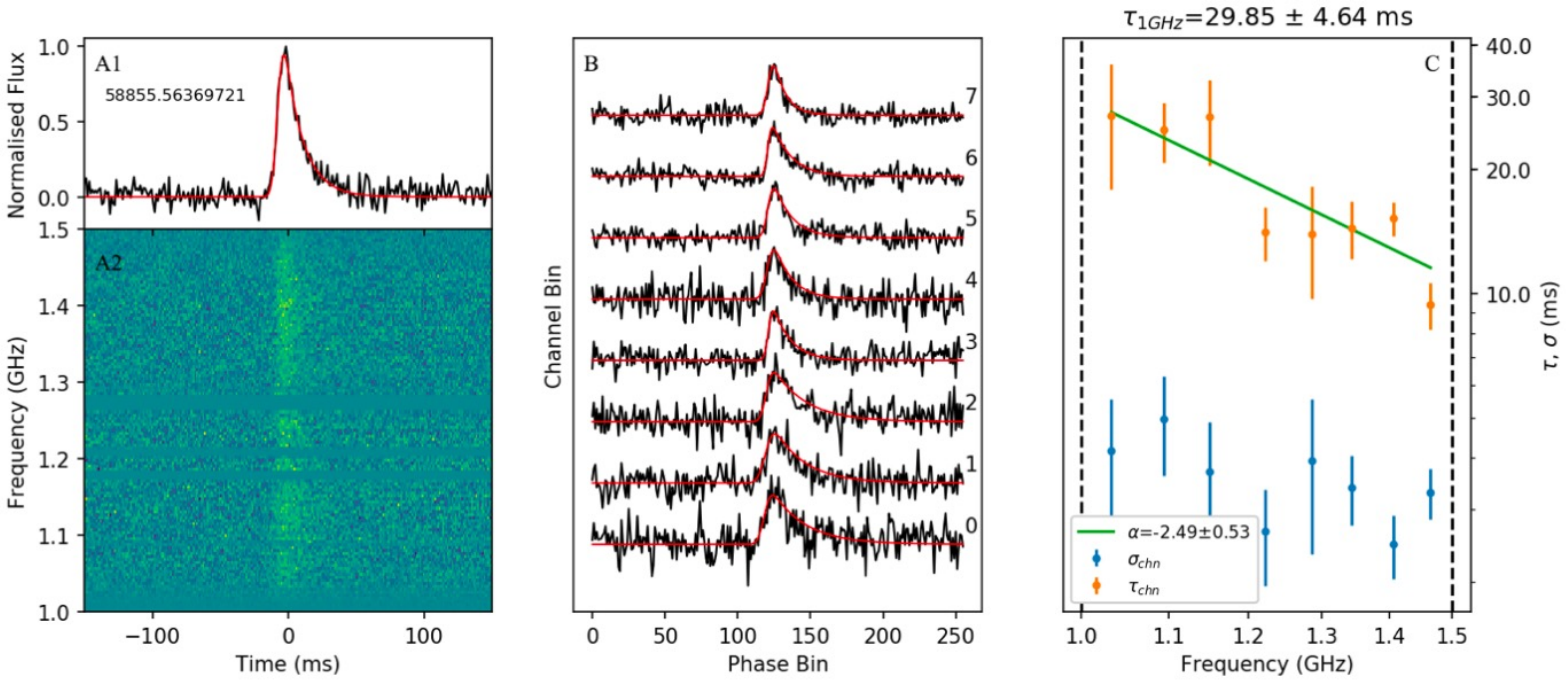

Pulse No. 24. **A1** and **A2** show the pulse profile and dynamical spectra, respectively. **B**: fitting of sub-band profile which with $S/N \geq 7$. **C**: scattering timescales as a function of frequency. The fitting parameters α, σ_{chn}, τ_{chn} and their 1σ errors are plotted.

Detail on pulse #41

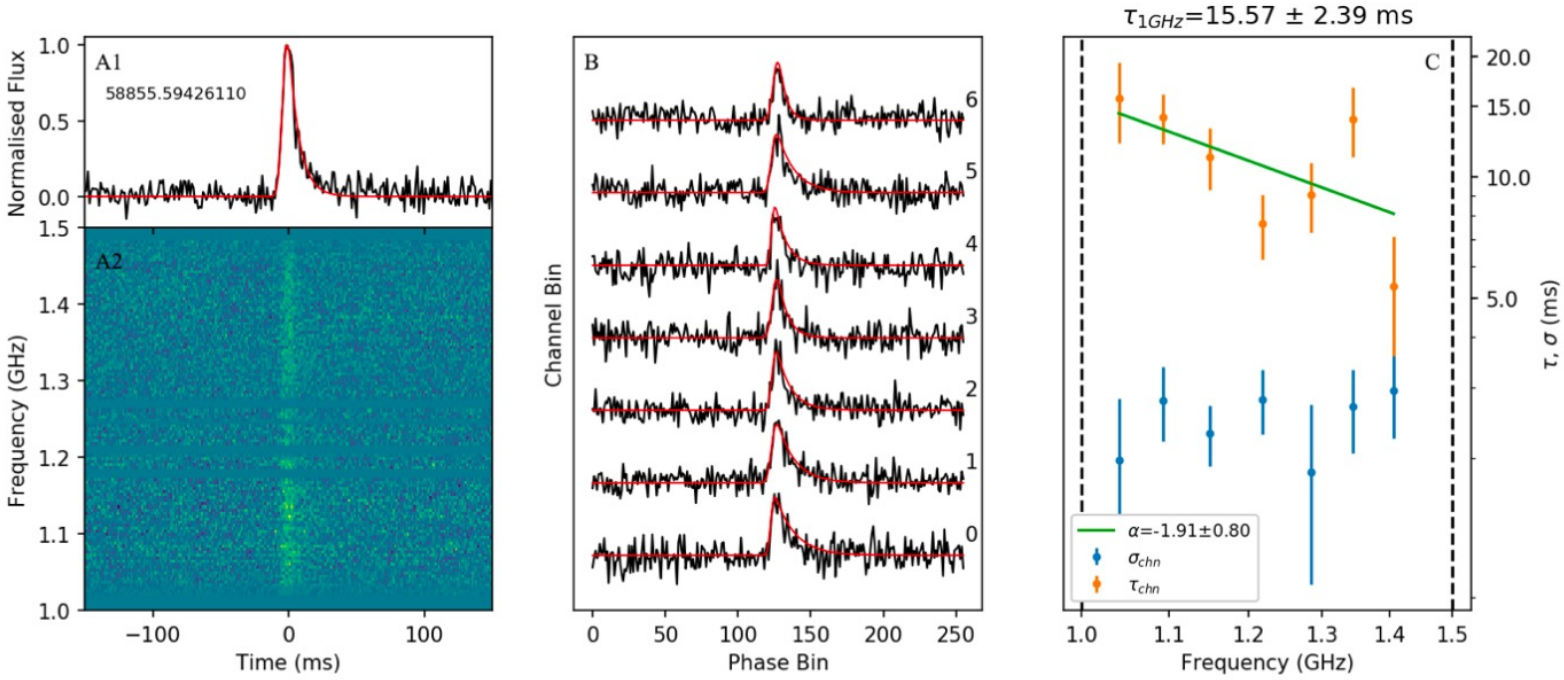

Pulse No. 41. **A1** and **A2** show the pulse profile and dynamical spectra, respectively. **B**: fitting of sub-band profile which with $S/N \geq 7$. **C**: scattering timescales as a function of frequency. The fitting parameters α, σ_{chn}, τ_{chn} and their 1σ errors are plotted.

Considerations on single pulse fitting

Linear regression of the scattering timescales shows their scattering timescale at 1 GHz of τ_{1GHz}=29.85±4.64 ms, 15.57±2.39 ms and a frequency scaling index of α=-2.49±0.53, and −1.91 ± 0.80 for the two pulses, respectively.

The scattering by the ionized plasma leads to the pulse being asymmetrically broader at lower frequencies. For the thin-screen scattering model, we could expect scaling indexes of -4 and -4.4, for Gaussian and Kolmogorov inhomogeneities, respectively .

However, note that deviations from the theoretical models had been already reported in several pulsars (e.g. PSR B0823+26, PSR B1839+56, and others): It was suggested that lower α values could result from limitations of the thin-screen model or from an anisotropic scattering mechanism.

The distribution of the ionized plasma around LS I +61◦ 303 cannot be an infinite thin screen, and should deviate from either Gaussian or Kolmogorov inhomogeneous distribution.

From another nearby pulsar?

- the angular resolution (L-band) of *FAST* is of ∼ 2.9 arcmin.
- As for other *FAST* observations in the same band, we cannot therefore formally exclude the presence of a pulsar just behind LS I +61° 303, unrelated to it, that is responsible for the pulsed emission.
- [This same applies to all other transient detection in this and other telescopes, of course]
- But..

From another nearby pulsar?

- On the one hand, if the emission would come from secondary lobes from a pulsar far away the field of LS I +61 303 (∼6 − 8’), the intrinsic flux density should be about ∼ 1000 times brighter than the detected level, i.e. about ∼ 10 − 100 Jy. Other telescopes could have easily detected the signal already.

From another nearby pulsar?

- On the one hand, if the emission would come from secondary lobes from a pulsar far away the field of LS I +61 303 (∼6 − 8’), the intrinsic flux density should be about ∼ 1000 times brighter than the detected level, i.e. about ∼ 10 − 100 Jy. Other telescopes could have easily detected the signal already.

- On the other hand, we simulated sets of Galactic positions of putative pulsars (which should also able to produce) magnetar flares and measure which is the random coincidence between these and our source of interest (so that both sources lie within 3 arcmin).

- We do so respecting the spatial distribution of the current population of pulsars in Galactic longitude and latitude.

- Using simulations of 1928 objects, the average number of simulated coincidences between the position of one of them and LS I +61 303 would still be ∼ 0.00093 (standard deviation 0.0304).

Why 1928?
-This is the actual number of known pulsars with |b| < 5 degrees
-We considered that future samples will contain such a number of magnetars. This is indeed conservative: this number is a factor of > 60 beyond the magnetars currently known, or a factor of ~2 larger than all pulsars expected to be detected anew by *FAST*, or even a factor of 4 larger than the number of magnetars born in the Galaxy in the last 25 kyr assuming the most favorable birth rate .